energies

MDPI

Article

A Novel Model of Counter-Current Imbibition in Interacting Capillaries with Different Size Distribution

Zhenjie Zhang [1,2], Tianyi Zhao [1,3] and Qingbang Meng [1,2,*]

[1] State Key Laboratory of Shale Oil and Gas Enrichment Mechanisms and Effective Development, SINOPEC, Beijing 100083, China
[2] School of Earth Resources, China University of Geosciences, Wuhan 430074, China
[3] SINOPEC Petroleum Exploration and Production Research Institute, Beijing 100083, China
* Correspondence: mengqb@cug.edu.cn

Abstract: The imbibition phenomenon widely exists in nature and industrial applications. It is of great significance to study the mechanism of imbibition and the influence laws of related factors. In this paper, based on the assumption of interacting capillaries, a capillary bundle model of counter-current imbibition is established. In addition, the characteristics of imbibition and the influences of capillary size and fluid viscosity are analyzed. The results show that water is imbibed into the smaller capillaries and expelled from the larger capillaries. The rate of the meniscus in water-imbibition capillaries is proportional to the square root of time. In the interacting capillaries, oil production by counter-current imbibition decreases and then increases gradually with the increase of the capillary diameter difference. When the total cross-sectional area of the capillary remains unchanged, the cross-sectional area of the total water-imbibition capillaries is affected by the size distribution of the capillaries. The larger the viscosity of the non-wetting phase, the more uneven the imbibition front, the lower the imbibition efficiency. The higher the viscosity of the wetting phase, the more uniform the imbibition front, and the higher the imbibition efficiency.

Keywords: multiphase flow; spontaneous imbibition; capillary pressure; pore size distribution

Citation: Zhang, Z.; Zhao, T.; Meng, Q. A Novel Model of Counter-Current Imbibition in Interacting Capillaries with Different Size Distribution. *Energies* **2022**, *15*, 6309. https://doi.org/10.3390/en15176309

Academic Editor: Hossein Hamidi

Received: 26 July 2022
Accepted: 24 August 2022
Published: 29 August 2022

1. Introduction

The problem of the basic dynamic and static process of porous media imbibition has always been a hot topic in geothermal, petroleum, coal, and other engineering and scientific research [1]. In porous media, the non-wetting phase is replaced by the wetting phase by capillary force; this is called imbibition, and it is a universal phenomenon in many engineering and scientific fields [2–5]. In the study of multiphase flow in porous media, imbibition oil recovery is always a very active field [6–8].

Numerous experimental and theoretical studies have explored the underlying mechanisms of imbibition in porous media and demonstrated that the rate and effect of imbibition are primarily affected by matrix and fluid properties control. Many factors affect the imbibition recovery factor, such as fluid properties, the microstructure of porous media, and fluid–solid coupling relationship [3,9]. There are many influencing factors of imbibition, and the imbibition mechanism is complex. As a matter of fact, the oil recovery by imbibition is related to many factors including interfacial tension, [10] pore geometry, [4,8,11] wettability, [12–15] shape, [16–18] liquid viscosity, [19–23] relative permeability, [21,24], and matrix boundary conditions [25–28]. The imbibition rate mainly depends on the fluid properties, rock properties, and the interaction between the rock–fluid [29]. Twenty years ago, Morrow and Mason reviewed the development of spontaneous imbibition and summarized the work of spontaneous imbibition in the 20th century [30]. They considered different wettability could affect different imbibition forms in different rock areas. Zhou et al. [31] believed that the capillary imbibition mechanism was an important basis for evaluating the wettability kinetics of brine/oil/rock systems. Xie and Morrow [32] presented that change

in wettability leaded to a decrease in capillary force and an order of magnitude decrease in imbibition rate. Many factors affect recovery by spontaneous imbibition, which is the condition to understand the influence of wettability on imbibition. Many studies have shown that initial water saturation, fluid, and rock interactions affect rock wettability [33].

As a significant parameter, fluid viscosity affects oil production rate and oil recovery [34,35]. Ma and Zhang et al. found that the residual oil had no significant change when the oil–water viscosity ratio was 1–170 by imbibition experiment. Using limestone samples, Hamidpour et al. [36] obtained similar results. Chatzis et al. [37] found that the imbibition rate decreased as the wet-phase viscosity increased and the final oil recovery was similar. Meng et al. [38] conducted imbibition experiments using porous media made of different fillers. It was found that final imbibition recovery rate of porous media filled with a more regular shape and a small particle size distribution was much higher than that filled with irregular shape and large particle size distribution. In porous media filled with regular shape and small particle size distribution, oil–water viscosity had no significant effect on the final recovery. However, in another porous medium, with the increase of oil–water viscosity, the imbibition recovery decreased obviously. Moreover, Meng et al. [19] proposed that different rock pore structures and pore size distributions in porous media are the reasons for different final recovery factors.

Imbibition characteristics as well as the influence of pore structure and fluid characteristics at different scales have been studied, which are the key to solving the effect of imbibition in engineering and guiding practice. In porous media, the topology of the pore structure is complex, and the flow between different pores interferes with each other. Dong [39] proposed a dual-capillary ideal connectivity model, assuming unimpeded flow between capillaries in the single-phase region. Ruth and Bartley [40] improved this theory to allow cross-flow with no pressure drop ("perfect cross-flow") between many tubes. Dong [41] deduced the fluid model and water fraction expression of two capillaries model with different diameters interacting with each other and established a model for analyzing immiscible displacement processes in porous media by interacting capillary bundles. It is found that the imbibition effect of the model is completely consistent with the experimental results, which further verifies the accuracy of the interaction capillary model. Dong [42] compared the displacement curves of interacting and non-interacting capillary bundle models. The effects of capillary force, injection rate, and oil–water viscosity ratio on the propulsion of oil–water meniscus in different capillaries were calculated. Unsal [43–45] used non-axisymmetric tubes to illustrate the basic principles of imbibition in tubes, verifying the accuracy of the ideal interacting capillaries model.

As mentioned above, many scholars have performed a lot of work on the mechanism and influencing factors of imbibition. However, due to the complex internal mechanism of imbibition, many influencing factors, and the complex pore structure of porous media, the imbibition mechanism between different pores is complex, and the imbibition mechanism under different pore distributions is unclear. The models proposed by predecessors cannot handle counter-current imbibition in the porous media [39–42]. Therefore, in this paper, based on the previous work on co-current imbibition, an interacting capillary model considering different size distributions is established to study the complex imbibition mechanism of porous media with different pore size distributions. The novel model can describe the mechanism of counter-current imbibition fundamentally and efficiently. In addition, the effect of capillary size distribution and fluid viscosity on counter-current imbibition was studied as well.

2. Mathematical Model and Numerical Calculation

In this work, it is assumed that the front of the wetting phase exists only on one side of the capillary. The effect of gravity was ignored and the parallel connection of three capillaries was considered. The diameter of the capillaries is different. The schematic diagram of the model is shown in Figure 1. In this model, the line represents the boundary of two capillaries, and the dashed line indicates that the capillaries are connected to each

other. If the fluid in the two capillaries is the same, there is no pressure difference between the two capillaries on the same section. The solid line represents that the interface fluid cannot pass through. The model is divided into three zones. The pressure distribution and water or oil saturation is different in different zones. In zone 1, water saturation is highest, thus, the gradient of pressure drop in water is lowest and gradient of pressure drop in oil is highest. The water saturation and pressure distribution can be analyzed similarly as well, as showed in Figure 1. The oil phase will flow out from the largest capillary, and the capillary back pressure is p_{c1}. This paper simulates the process of minimal capillary imbibition to the bottom.

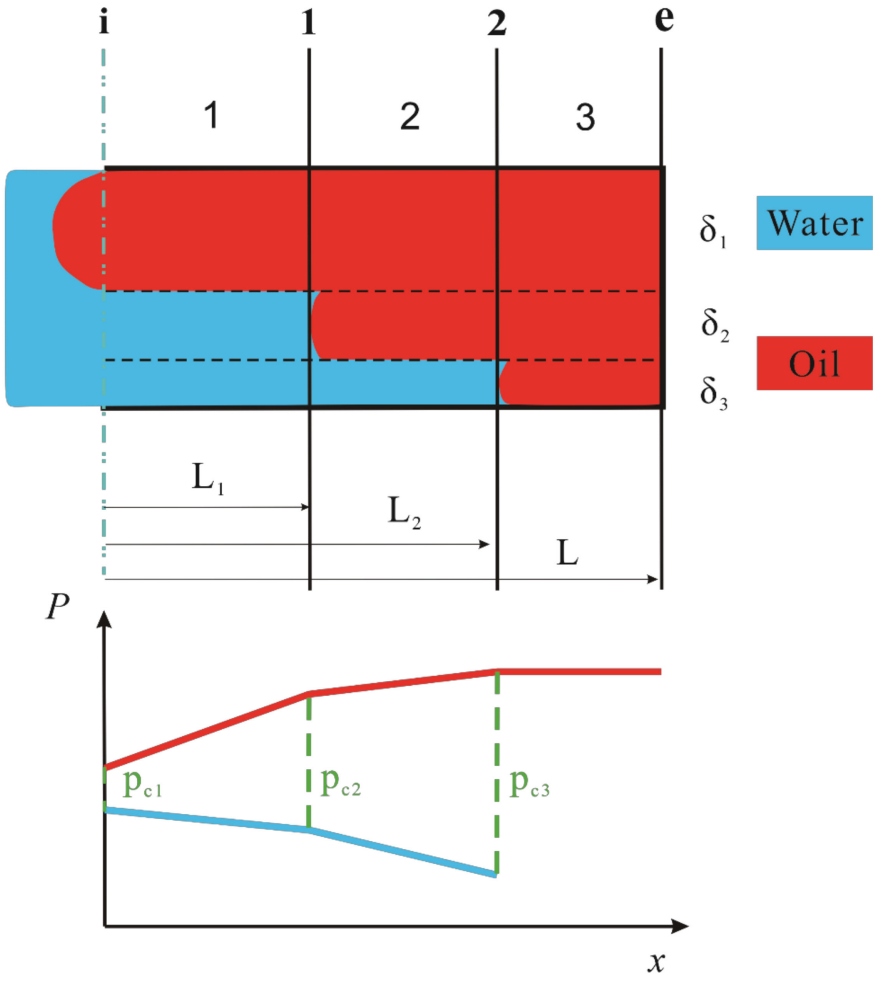

Figure 1. Schematic diagram of fluid distribution and pressure distribution in reverse imbibition of three interacting capillaries. "i" represents the inlet of capillary model and e represents the end of capillary model. δ_1, δ_2, and δ_3 are the diameters of the three capillary tubes.

According to the distribution characteristics of the fluid, the capillary model divides the imbibition process into three regions by the imbibition front in the capillaries. It is assumed that the single-phase in any capillary is controlled by the Hagen–Poiseuille expression [40]:

$$Q_\alpha = \frac{\pi\delta^4}{128\mu_\alpha}\frac{dP_\alpha}{dx} \quad (1)$$

where Q is the flow rate of fluid in different capillaries, δ is the diameters of the capillary, μ is viscosity for different flow, P is pressure in fluid, x is the distance, α represents the phase.

The flow in each region is governed by the following expressions, which are obtained by summing the flows in the capillaries in the region, separately by phase (Figure 1):

$$Q_{w1} = \frac{\pi(P_{wi} - P_{w1})}{128\mu_w L_1}(\delta_2^4 + \delta_3^4) \tag{2}$$

$$Q_{o1} = \frac{\pi(P_{oi} - P_{o1})}{128\mu_o L_1}\delta_1^4 \tag{3}$$

$$Q_{w2} = \frac{\pi(P_{w1} - P_{w2})}{128\mu_w (L_2 - L_1)}\delta_3^4 \tag{4}$$

$$Q_{o2} = \frac{\pi(P_{o1} - P_{o2})}{128\mu_o (L_2 - L_1)}(\delta_1^4 + \delta_2^4) \tag{5}$$

$$Q_{o3} = \frac{\pi(P_{o2} - P_{oe})}{128\mu_o (L - L_2)}(\delta_1^4 + \delta_2^4 + \delta_3^4) \tag{6}$$

where Q_{w1} and Q_{w2} are the flow rate wetting phase, m^3/s; Q_{o1}, Q_{o2}, and Q_{o3} are flow rate of the non-wetting phase, m^3/s; μ_w and μ_o are the wetting phase, and non-wetting phase fluids, Pa s; P_w and P_o are the pressures of the wetting and non-wetting phases at the imbibition front, Pa; P_{wi} is the inlet pressure of the wetting phase, Pa; L is the capillary length, m; L_1 and L_2 are the distance between the imbibition front and the inlet end of the wetting phase, m; δ_1, δ_2, and δ_3 are the diameters of the five capillary tubes, m.

The relationship between capillary pressure and oil–water two-phase pressure is:

$$P_{cj} = P_{oj} - P_{wj} \tag{7}$$

where P_{cj} is capillary pressure, Pa; P_{oi} is the non-wetting phase pressure near the imbibition front of the j capillary, Pa; P_{wi} is the wetting-phase pressure near the imbibition front of the j capillary, Pa; j is the capillary code, which is equal to 1, 2, or 3.

Capillary pressure can be expressed as:

$$P_{cj} = \frac{4\sigma\cos\theta}{\delta_j} \tag{8}$$

where σ is the interfacial tension, N/m; θ is the contact angle.

Through the continuity equation, the total flow in each zone can be obtained:

$$Q_t = Q_{wj} + Q_{oj} \tag{9}$$

The imbibition model is obtained by modeling the continuity equation, and Equations (2)–(9) are simultaneously obtained:

$$Q_t\frac{L_1}{\lambda_{o1} + \lambda_{w2} + \lambda_{w3}} - \frac{\lambda_{o1}}{\lambda_{o1} + \lambda_{w2} + \lambda_{w3}}(P_{c1} - P_{c2}) = P_{wi} - P_{w1} \tag{10}$$

$$Q_t\frac{L_2 - L_1}{\lambda_{o1} + \lambda_{o2} + \lambda_{w3}} - \frac{\lambda_{o1} + \lambda_{o2}}{\lambda_{o1} + \lambda_{o2} + \lambda_{w3}}(P_{c2} - P_{c3}) = P_{w1} - P_{w2} \tag{11}$$

$$Q_t\frac{L - L_2}{\lambda_{o1} + \lambda_{o2} + \lambda_{o3}} - (P_{c3} - P_{oe}) = P_{w2} \tag{12}$$

where

$$\lambda_{\alpha j} = \frac{\pi}{128\mu_\alpha}\delta_j^4 \tag{13}$$

This set of four equations contains eight unknowns: Q_t, P_{wi}, P_{w1}, P_{w2}, P_{oe}, L_1, L_2, L_3. This system of equations will allow for two boundary conditions. These are usually Q_t, P_{wi},

as well as P_{oe}, all possibly as a function of time. Given two of these quantities, the third quantity can be obtained by summing the governing equations:

$$Q_t\left[\frac{L_1}{\lambda_{o1}+\lambda_{w2}+\lambda_{w3}}+\frac{L_2-L_1}{\lambda_{o1}+\lambda_{o2}+\lambda_{w3}}+\frac{L-L_2}{\lambda_{o1}+\lambda_{o2}+\lambda_{o3}}\right]-\frac{\lambda_{o1}}{\lambda_{o1}+\lambda_{w2}+\lambda_{w3}}(P_{c1}-P_{c2}) \\ -\frac{\lambda_{o1}+\lambda_{o2}}{\lambda_{o1}+\lambda_{o2}+\lambda_{w3}}(P_{c2}-P_{c3})-P_{c3}+P_{oe}=P_{wi} \tag{14}$$

In the next step, the distance can be calculated as follows.

$$L_j{}' = L_j + \Delta L_j \cdot dt \tag{15}$$

where ΔL_j is the format of the expression,

$$\Delta L_j = \frac{dL_j}{dt} = \frac{4(Q_{wj}-Q_{wj+1})}{\pi\delta_j^2} \tag{16}$$

For the present paper, the size of a time step (d_t) was calculated as the interval required for the fluid in the most advanced interface to move a given distance ΔL. The specific flowchart is shown in Figure 2.

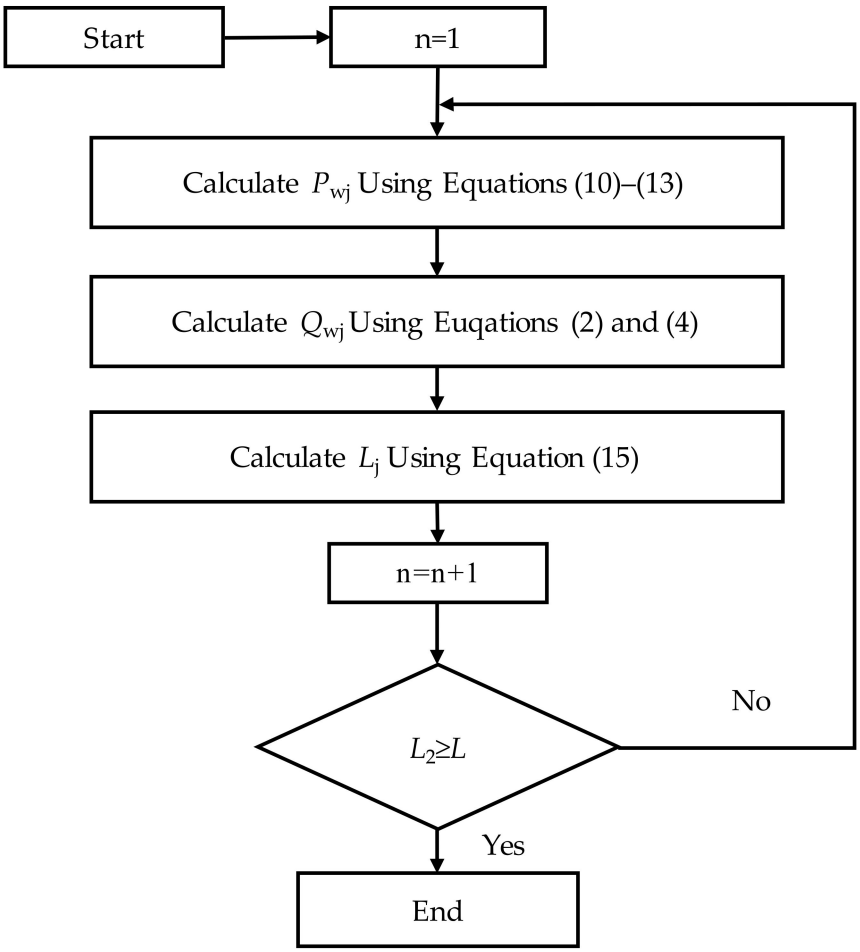

Figure 2. Flowchart of three capillary model calculations. P_{wj} is the wetting-phase pressure near the imbibition front of the j capillary, Q_{wj} is the flow rate of wetting phase in j capillary, L_j is the advancing distance by water in j capillary.

3. Results and Discussion

3.1. Parameter Values and Characteristics of the Base Case

In this paper, the imbibition mechanism of the interacting capillary model is first analyzed. Then, the influence of the capillary size distribution and fluid viscosity on counter-current imbibition is analyzed. For the basic model, the initial boundary condition is $Q_t = 0\ m^3/s$, $P_{wi} = 0$ Pa to define the model as spontaneous imbibition. Other specific parameters are shown in Table 1.

Table 1. Basic parameters of the three interaction capillary models.

Parameters	Values	Parameters	Values
L (Core Length)	0.1 m	σ (Interfacial Tension)	32 mN/m
δ_1 (NO. 1 Capillary Diameter)	60×10^{-6} m	θ (Contact Angle)	0
δ_2 (NO. 2 Capillary Diameter)	40×10^{-6} m	L_1 (L_1 Initial Value)	0.00001 m
δ_3 (NO. 3 Capillary Diameter)	20×10^{-6} m	L_2 (L_2 Initial Value)	0.00002 m
μ_w (Wetting Phase Viscosity)	1 mPa·s	d_t (Time Step)	0.00001 s
μ_{nw}(Non-wetting Phase Viscosity)	1 mPa·s		

It can be seen that the advancing distance of the imbibition front of the small capillary is always larger than that of the large capillary model (Figure 3), and the difference between the advancing distances of the two capillaries has been increasing with imbibition. The results of the model are consistent with the lattice Boltzmann method (LBM) on counter-current imbibition [46–48]. It is found that the minimum capillary imbibition rate V3 is always greater than the second capillary imbibition rate V2 (Figure 4). The imbibition rate is related to the pressure difference of the imbibition front, the radius of the capillary, and the distance of imbibition. The pressure difference of the imbibition front is a fixed value, and the radius of the capillary is also a fixed value. These factors determine that V3 is greater than V2. In addition, the imbibition speed is related to the displacement. The advancing distance of the imbibition front gradually increases, and the resistance increases, which leads to the gradual decrease of the advancing speed of the imbibition front.

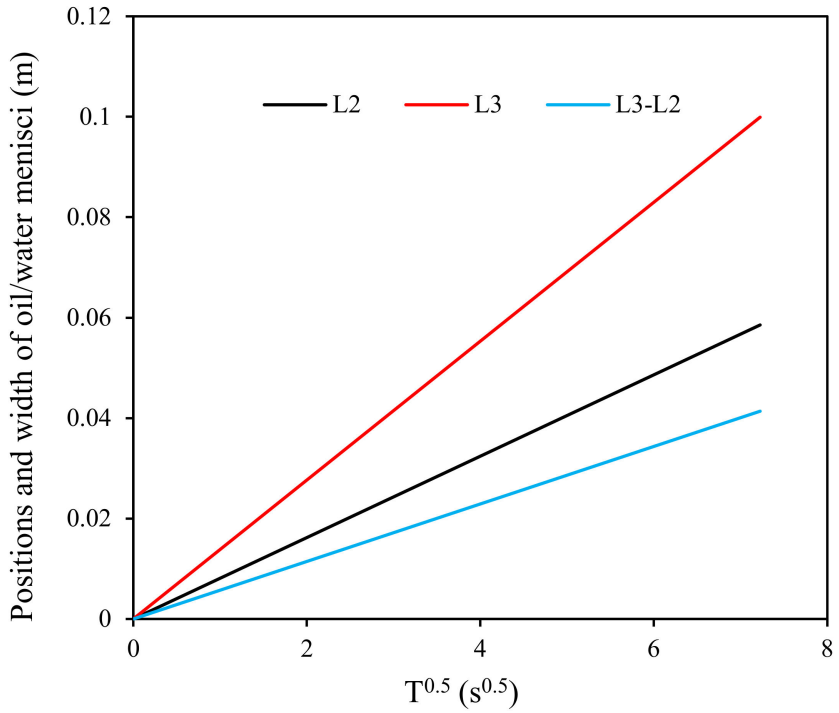

Figure 3. Variation of the imbibition front of two smaller capillaries.

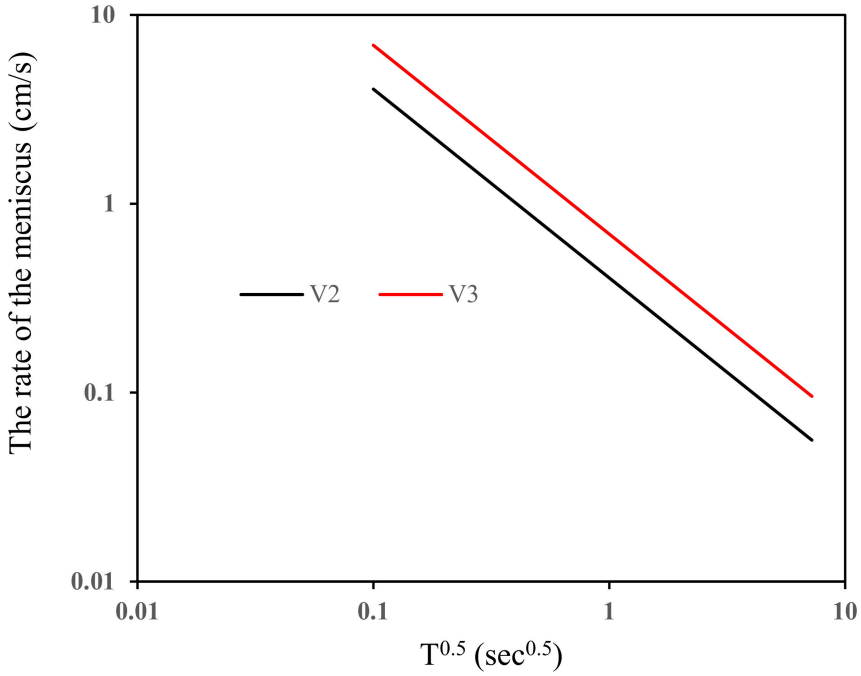

Figure 4. Variation of the advancing rate of two smaller capillaries.

3.2. Effect of Capillary Size Distribution

The imbibition recovery factor is calculated by dividing oil production by total oil when the water in the smallest capillary reached the end of capillary. It can be seen that the amount of imbibition decreases and then increases gradually with the increase of the capillary diameter difference, and the imbibition amount is the smallest at 15 μm (Figure 5). This is because the difference between the imbibition fronts in the two advancing capillaries gradually increases with the increase of the difference of capillary diameter during the imbibition process, and the phenomenon of imbibition fingering is becoming more and more obvious. When the minimum capillary imbibes to the bottom end, the advancing distance of the imbibition front of the other capillary becomes shorter and the imbibition amount decreases.

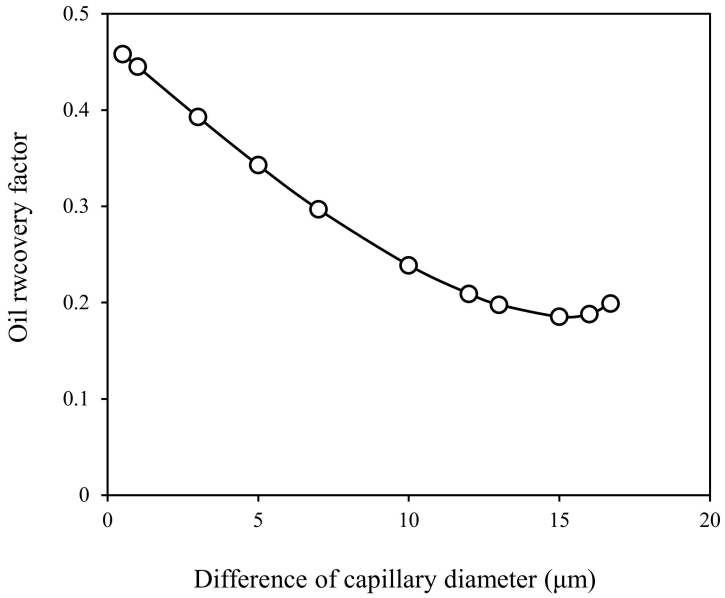

Figure 5. Relationship between imbibition recovery factor and capillary size distribution.

The amount of imbibition is related to the imbibition distance and the size distribution of the capillary. Therefore, the imbibition effect first becomes worse and then becomes better. The imbibition time first decreases and then increases with the increase of the uniformity of the capillary size (Figure 6). This is because the imbibition time depends on the time when the smallest capillary reaches the bottom of the capillary. The capillary imbibition time is related to the size of the capillary and the energy of the capillary imbibition; that is the pressure difference. When the capillary size distribution range is large, on the one hand, as the capillary size difference decreases, the difference between the minimum capillary imbibition pressure and the maximum capillary back pressure decreases, which leads to a decrease in the imbibition rate; on the other hand, the increase in the size of the smallest capillary leads to an increase in the imbibition rate. The decrease of capillary imbibition time is the result of two factors. However, with the further decrease of the capillary size difference, the imbibition pressure difference further decreases, and the increase of the minimum capillary diameter has little effect on the imbibition rate. Therefore, the imbibition time showed an increasing trend.

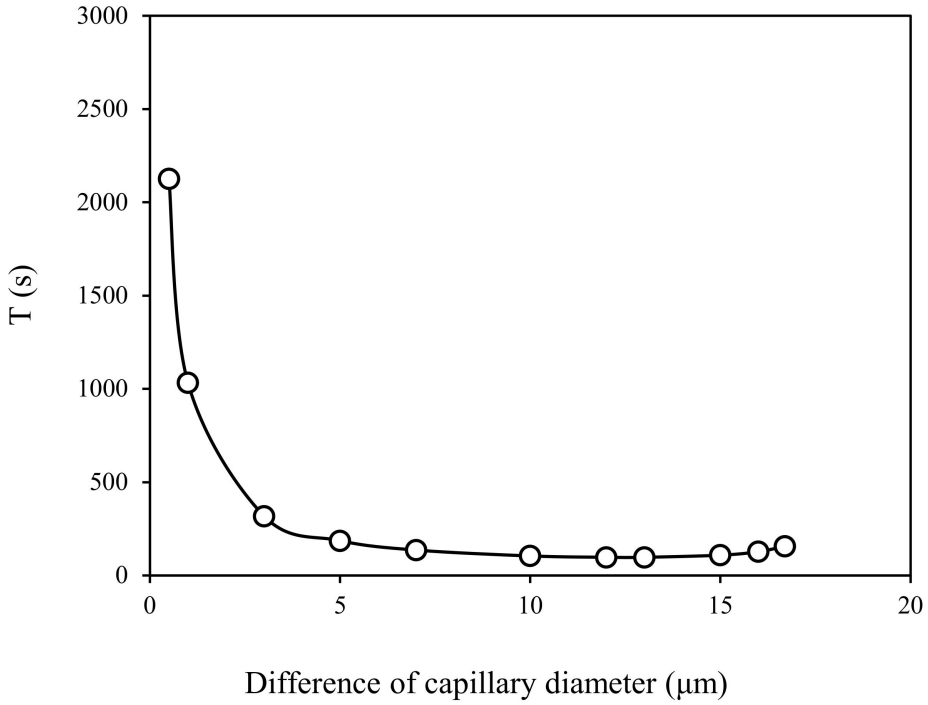

Figure 6. Relationship between imbibition time and capillary size distribution.

3.3. Effect of Viscosity

The influence of viscosity is observed by changing the non-wetting phase viscosity when the wetting phase viscosity is 1 mPa·s (Figures 7 and 8). With the increase of the non-wetting phase viscosity, the imbibition recovery factor becomes lower and lower. The trend of decreasing imbibition amount is slowed down when the non-wetting phase viscosity is greater than 100 mPa·s. The imbibition time increases with the viscosity of the non-wetting phase. The difference between the capillary imbibition fronts is small as the viscosity of the non-wetting phase becomes small, and the interface of the imbibition front is relatively uniform. Therefore, the imbibition effect is better and the imbibition amount is high. This is because imbibition always chooses a way with less energy consumption to advance in the capillary. The longer the wetting phase fluid in the small capillary, the greater the energy consumption. Since the non-wetting phase viscosity is lower, the resistance is lower, so the imbibition time is shorter. As the viscosity of the non-wetting phase increases, the imbibition fingering phenomenon becomes more obvious, and the imbibition effect becomes worse. When the non-wetting phase viscosity increases to a certain value,

imbibition amount does not decrease. This is because the main imbibition amount comes from the imbibition of the smallest capillary, the effect of the reduced imbibition amount of the remaining capillaries is not obvious.

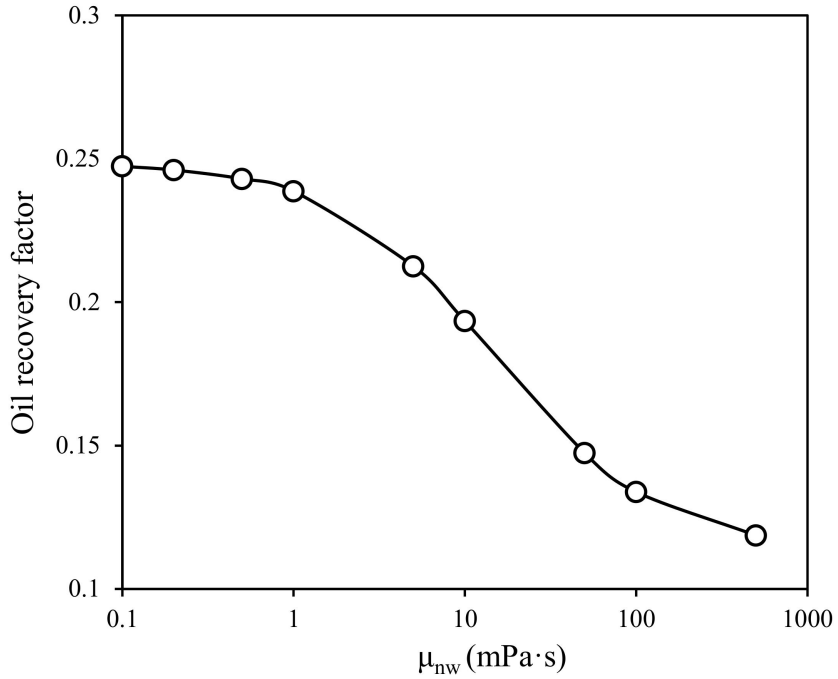

Figure 7. Oil recovery factor of different non-wetting phase viscosities of three interacting capillaries.

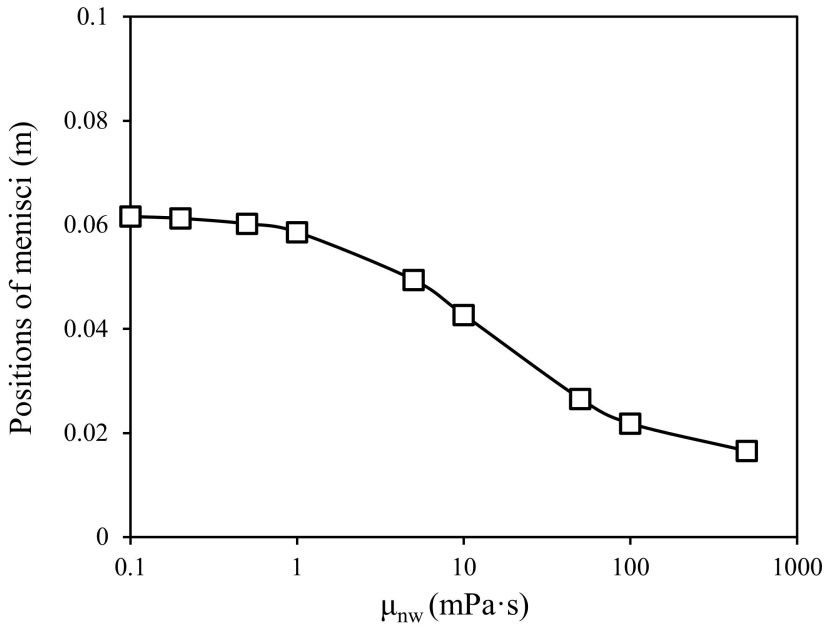

Figure 8. The positions of menisci of different non-wetting phase viscosities of three interacting capillaries.

In addition, the influence of non-wetting phase viscosity is studied by changing the number of capillaries. It is found that the non-wetting phase viscosity increases, the imbibition distance of other capillaries becomes smaller, and the heterogeneity of the imbibition front becomes worse when the smallest capillary imbibes to the bottom end (Figure 9). As the viscosity of the non-wetting phase increases, the imbibition time increases. This is because the increase of non-wetting phase viscosity leads to the increase of viscous force. Therefore, the increase of imbibition resistance increases the time of imbibition.

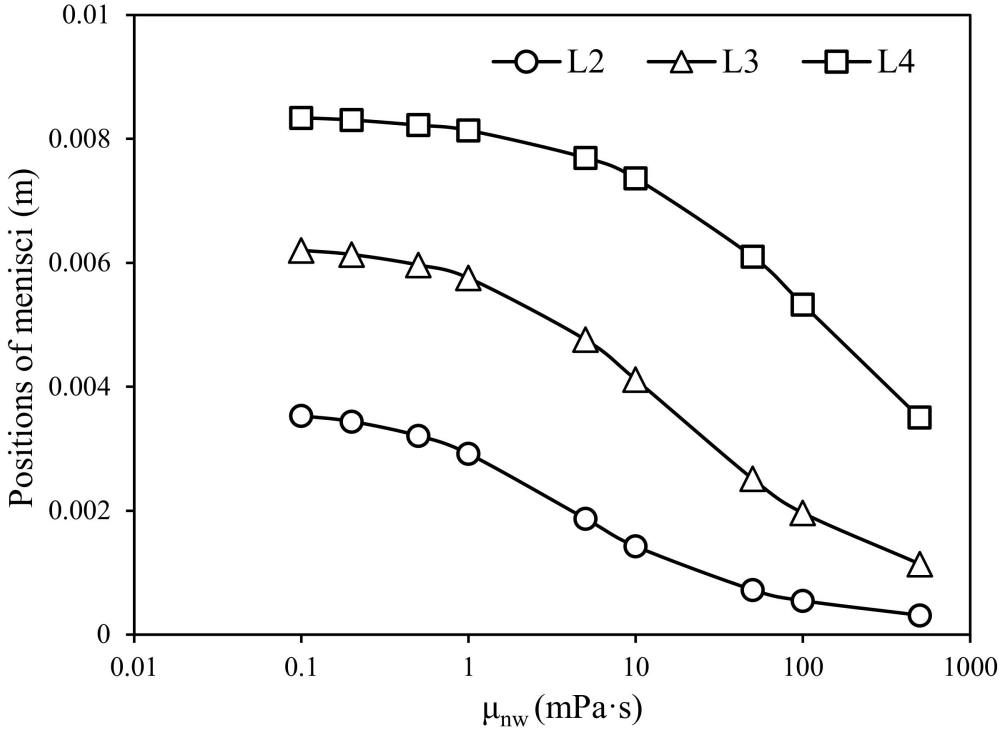

Figure 9. The positions of menisci of imbibition capillaries under different non-wetting phase viscosities (μ_w = 1 mPa·s).

The effect of the viscosity of the wetting phase is studied when the viscosity of the non-wetting phase is 10 mPa·s, and the results are shown in Figures 10 and 11. As the viscosity of the wetting phase increases, the amount of imbibition increases. When the wetting phase viscosity is greater than 10 mPa·s, the amount of imbibition increases slowly, and the imbibition time increases. The difference between the capillary imbibition fronts is large when the viscosity of the wetting phase is small, and the fingering phenomenon of the imbibition front is obvious. Therefore, the imbibition effect is poor, and the amount of imbibition is low. This is because the imbibition always chooses away with less energy consumption to advance in the capillary. The energy consumption of imbibition in the small capillary is small. Therefore, the imbibition in the small capillaries is fast, resulting in a larger difference between imbibition fronts and a lower imbibition recovery. Due to the lower viscosity of the wetting phase, the imbibition resistance is smaller. Thus, the imbibition time is shorter. As the viscosity of the wetting phase increases, the imbibition fingering phenomenon weakens and the imbibition effect becomes better. When the wetting phase viscosity increases to a certain value, the imbibition effect does not increase significantly. This is because the energy is mainly consumed in the wetting phase fluid and is negligible in the non-wetting phase fluid.

In addition, the influence of the viscosity of the wetting phase is studied by changing the number of capillaries. It is found that as the viscosity of the wetting phase increases, the imbibition distance of other capillaries becomes larger when the smallest capillary imbibes to the bottom end, and the heterogeneity of the imbibition front becomes better (Figure 12). The imbibition time increases with the increase of wetting phase viscosity. This is because the increase of wetting phase viscosity leads to the increase of viscous force. Therefore, the increase of imbibition resistance increases the time of imbibition.

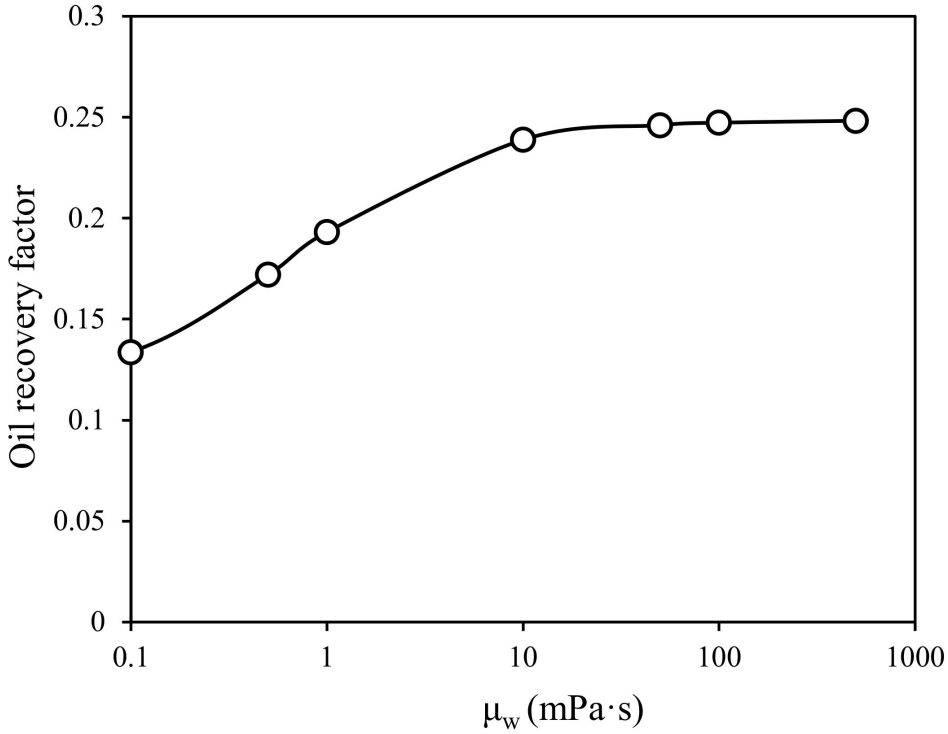

Figure 10. Oil recovery factor of different wetting phase viscosities of three interacting capillaries.

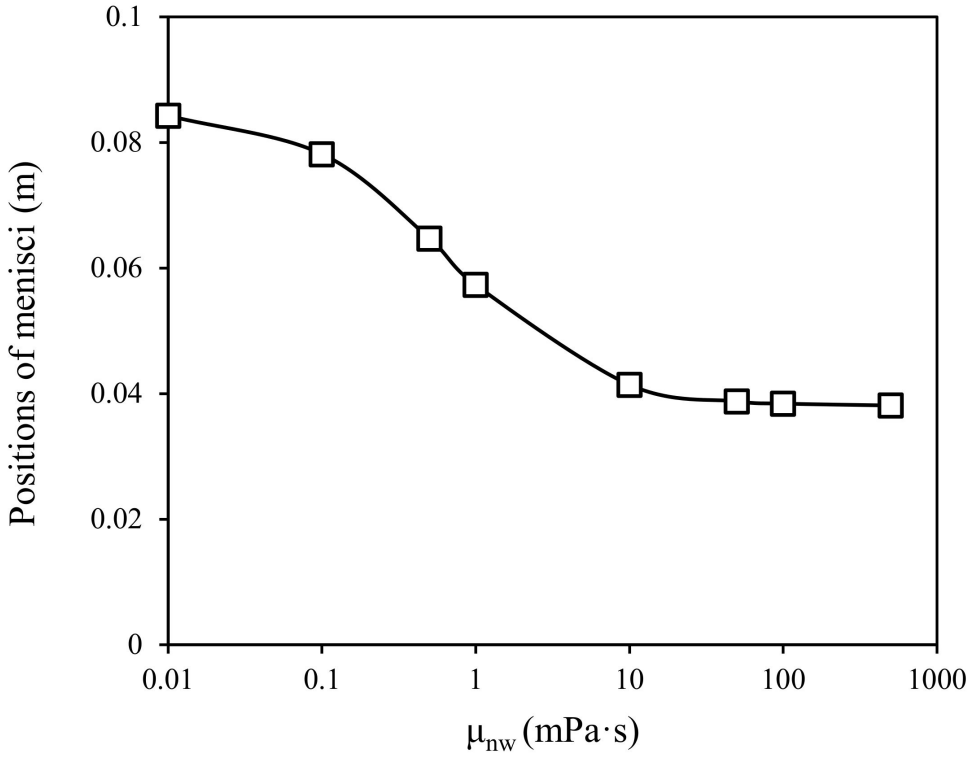

Figure 11. The positions of menisci of different wetting phase viscosities of three interacting capillaries.

In order to analyze the effect of viscosity ratio on imbibition, different viscosity ratio schemes of 0.1, 1, and 10 are designed, respectively. The imbibition results are shown in Figure 13. When the viscosity ratio is constant, the oil amount of imbibition is a certain value, which has nothing to do with the wetting or non-wetting viscosity. The viscosity only affects the rate of imbibition. When the viscosity ratio is small, the amount of oil

imbibition is higher. With the increase of viscosity ratio, the amount of imbibition decreases gradually (Figure 14).

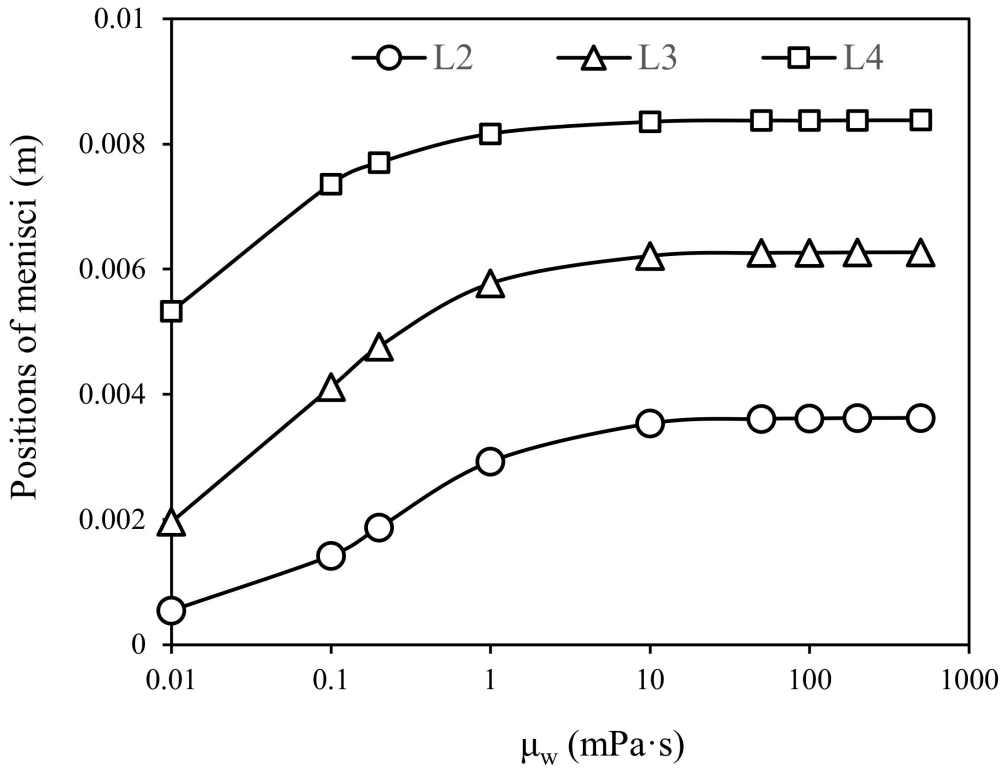

Figure 12. The positions of menisci of imbibition capillaries under different wetting phase viscosities (μ_{nw} = 1 mPa·s).

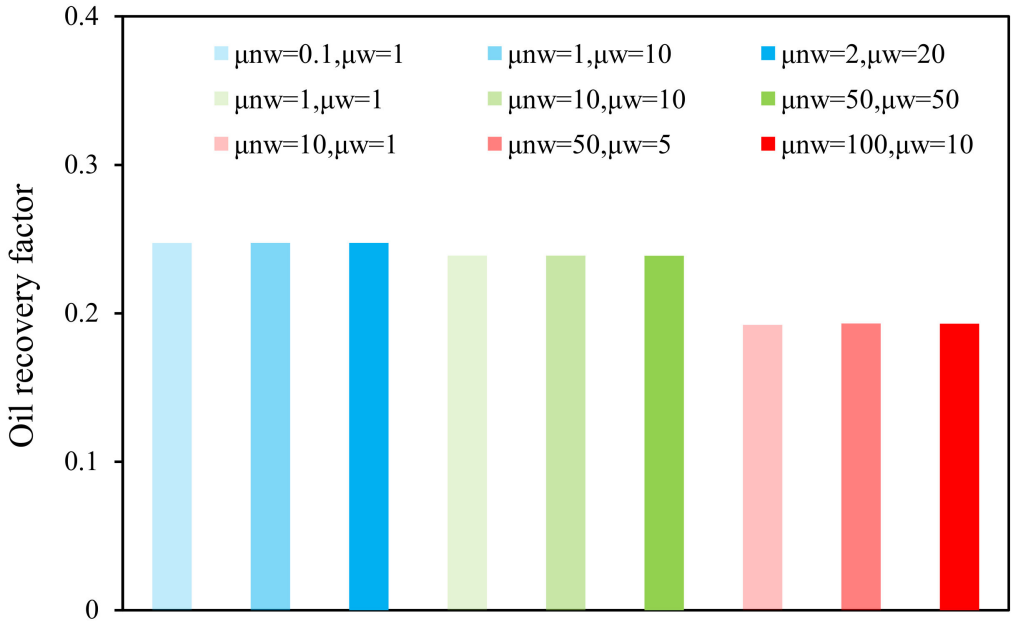

Figure 13. Oil recovery factor under different viscosity ratios (M = μ_{nw}/μ_w is 0.1 (blue), 1 (green), 10 (red).

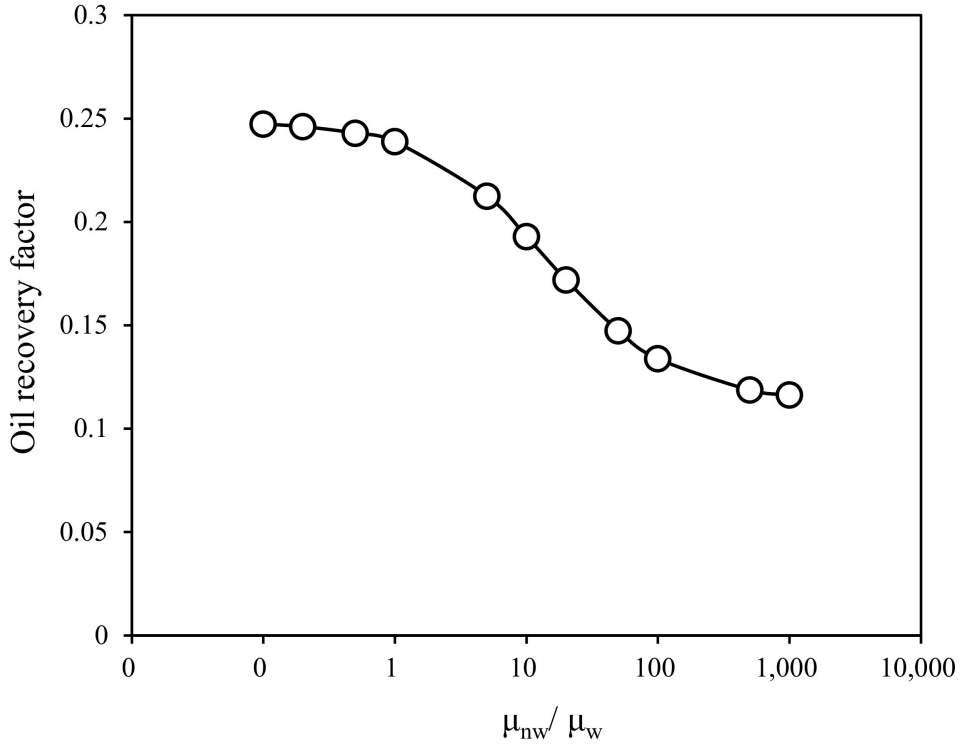

Figure 14. Diagram of the viscosity ratio of the imbibition amount of three interacting capillaries.

4. Conclusions

In this work, an interacting capillary model of counter-current imbibition is established. In addition, it can describe the mechanism of counter-current imbibition more simply, clearly, and efficiently. The mechanism of counter-current imbibition in capillaries with different size distributions is studied. The following conclusions can be obtained.

1. In the interacting capillary model, the wetting phase always preferentially enters the small capillaries. The pressure of the imbibition fronts during the imbibition process is fixed, and it is related to the capillary size and fluid properties. The advancing distance of the imbibition front is proportional to the square root of time.
2. The capillary size distribution has a complex impact on the counter-current imbibition. The amount of imbibition decreases and then increases gradually with the increase of the capillary diameter difference.
3. The imbibition efficiency decreases, and the imbibition time increases gradually with increasing the non-wetting phase viscosity. As the viscosity of the wetting phase increases, oil production by imbibition increases and the imbibition time increases gradually. The amount of imbibition is the same under the same viscosity ratio. The amount of imbibition decreases gradually with the increase of the viscosity ratio.

Author Contributions: Formal analysis, writing: original draft, Z.Z.; Conceptualization, methodology, T.Z.; supervision, writing: review and editing, Q.M. All authors have read and agreed to the published version of the manuscript.

Funding: This research was funded by State Key Laboratory of Shale Oil and Gas Enrichment Mechanisms and Effective Development, the National Natural Science Foundation of China (No. 51804284).

Institutional Review Board Statement: Not applicable.

Informed Consent Statement: Not applicable.

Data Availability Statement: Not applicable.

Conflicts of Interest: The authors declare no conflict of interest.

References

1. Cai, J.; Jin, T.; Kou, J.; Zou, S.; Xiao, J.; Meng, Q. Lucas–Washburn equation-based modeling of capillary-driven flow in porous systems. *Langmuir* **2021**, *37*, 1623–1636. [CrossRef] [PubMed]
2. Li, C.; Singh, H.; Cai, J. Spontaneous imbibition in shale: A review of recent advances. *Capillarity* **2019**, *2*, 17–32. [CrossRef]
3. Meng, Q.; Liu, H.; Wang, J. A critical review on fundamental mechanisms of spontaneous imbibition and the impact of boundary condition, Fluid Viscosity and Wettability. *Adv. Geo-Energy Res.* **2017**, *1*, 1–17. [CrossRef]
4. Schmid, K.S.; Geiger, S. Universal scaling of spontaneous imbibition for water-wet systems. *Water Resour. Res.* **2012**, *48*, w03507. [CrossRef]
5. Wang, J.; Dong, M. Trapping of the Non-Wetting Phase in an Interacting Triangular Tube Bundle Model. *Chem. Eng. Sci.* **2011**, *66*, 250–259. [CrossRef]
6. Li, Y.; Morrow, N.R.; Ruth, D. Similarity solution for linear counter-current spontaneous imbibition. *J. Pet. Sci. Eng.* **2003**, *39*, 309–326. [CrossRef]
7. Velasco-Lozano, M.; Balhoff, M.T. Modeling of Early- and Late-Time Countercurrent Spontaneous Imbibition in Porous Media: A Semi-Analytical Approach. *J. Pet. Sci. Eng.* **2022**, *208*, 109499. [CrossRef]
8. Ramezanzadeh, M.; Khasi, S.; Ghazanfari, M.H. Simulating Imbibition Process Using Interacting Capillary Bundle Model with Corner Flow: The Role of Capillary Morphology. *J. Pet. Sci. Eng.* **2019**, *176*, 62–73. [CrossRef]
9. Meng, Q.; Liu, H.; Wang, J.; Zhang, H. Effect of wetting-phase viscosity on cocurrent spontaneous imbibition. *Energy Fuels* **2016**, *30*, 835–843. [CrossRef]
10. Shen, Y.; Ge, H.; Meng, M.; Jiang, Z.; Yang, X. Effect of water imbibition on shale permeability and its influence on gas production. *Energy Fuels* **2017**, *31*, 4973–4980. [CrossRef]
11. Li, K.; Horne, R.N. An analytical scaling method for spontaneous imbibition in gas/water/rock systems. *SPE J.* **2004**, *9*, 322–329. [CrossRef]
12. Ma, S.; Zhang, X.; Morrow, N.R.; Zhou, X. Characterization of wettability from spontaneous imbibition measurements. *J. Can. Pet. Technol.* **1999**, *38*, PETSOC-99-13-49. [CrossRef]
13. Yildiz, H.O.; Morrow, N.R. Effect of wettability on waterflood recovery for crude-oil/brine/rock systems. *J. Pet. Sci. Eng.* **1996**, *14*, 159–168. [CrossRef]
14. Seyyedi, M.; Sohrabi, M. Enhancing water imbibition rate and oil recovery by carbonated water in carbonate and sandstone rocks. *Energy Fuels* **2016**, *30*, 285–293. [CrossRef]
15. Li, C.; Shen, Y.; Ge, H.; Zhang, Y.; Liu, T. Spontaneous imbibition in fractal tortuous micro-nano pores considering dynamic contact angle and slip effect: Phase portrait analysis and analytical solutions. *Sci. Rep.* **2018**, *8*, 3919. [CrossRef]
16. Cai, J.; Yu, B. A discussion of the effect of tortuosity on the capillary imbibition in porous media. *Transp. Porous Media* **2011**, *89*, 251–263. [CrossRef]
17. Gao, L.; Yang, Z.; Shi, Y. Experimental study on spontaneous imbibition characteristics of tight rocks. *Adv. Geo-Energy Res.* **2018**, *2*, 292–304. [CrossRef]
18. Meng, Q.; Cai, Z.; Cai, J.; Yang, F. Oil recovery by spontaneous imbibition from partially water-covered matrix blocks with different boundary conditions. *J. Pet. Sci. Eng.* **2019**, *172*, 454–464. [CrossRef]
19. Meng, Q.; Liu, H.; Wang, J. Effect of viscosity on oil production by cocurrent and countercurrent imbibition from cores with two ends open. *SPE Reserv. Eval. Eng.* **2017**, *20*, 251–259. [CrossRef]
20. Ma, S.; Zhang, X.; Morrow, N.R. Influence of fluid viscosity on mass transfer between rock matrix and fractures. *J. Can. Pet. Technol.* **1999**, *38*, PETSOC-99-07-02. [CrossRef]
21. Abd, A.S.; Elhafyan, E.; Siddiqui, A.R.; Alnoush, W.; Blunt, M.J.; Alyafei, N. A Review of the Phenomenon of Counter-Current Spontaneous Imbibition: Analysis and Data Interpretation. *J. Pet. Sci. Eng.* **2019**, *180*, 456–470. [CrossRef]
22. Standnes, D.C.; Andersen, P.Ø. Analysis of the Impact of Fluid Viscosities on the Rate of Countercurrent Spontaneous Imbibition. *Energy Fuels* **2017**, *31*, 6928–6940. [CrossRef]
23. Babadagli, T. Temperature effect on heavy-oil recovery by imbibition in fractured reservoirs. *J. Pet. Sci. Eng.* **1996**, *14*, 197–208. [CrossRef]
24. Behbahani, H.S.; Di Donato, G.; Blunt, M.J. Simulation of counter-current imbibition in water-wet fractured reservoirs. *J. Pet. Sci. Eng.* **2006**, *50*, 21–39. [CrossRef]
25. Zhang, X.; Morrow, N.R.; Ma, S. Experimental verification of a modified scaling group for spontaneous imbibition. *SPE Reserv. Eng.* **1996**, *11*, 280–285. [CrossRef]
26. Ma, S.; Marrow, N.R.; Zhang, X. Generalized scaling of spontaneous imbibition data for strongly water-wet systems. *J. Pet. Sci. Eng.* **1997**, *18*, 165–178.
27. Yildiz, H.O.; Gokmen, M.; Cesur, Y. Effect of shape factor, characteristic length, and boundary conditions on spontaneous imbibition. *J. Pet. Sci. Eng.* **2006**, *53*, 158–170. [CrossRef]
28. Zhang, S.; Pu, H.; Zhao, J.X. Experimental and Numerical Studies of Spontaneous Imbibition with Different Boundary Conditions: Case Studies of Middle Bakken and Berea Cores. *Energy Fuels* **2019**, *33*, 5135–5146. [CrossRef]
29. Tian, W.; Wu, K.; Gao, Y.; Chen, Z.; Gao, Y.; Li, J. A Critical Review of Enhanced Oil Recovery by Imbibition: Theory and Practice. *Energy Fuels* **2021**, *35*, 5643–5670. [CrossRef]
30. Morrow, N.R.; Mason, G. Recovery of oil by spontaneous imbibition. *Curr. Opin. Colloid Interface Sci.* **2001**, *6*, 321–337. [CrossRef]

31. Zhou, X.M.; Torsaeter, O.; Xie, X.; Morrow, N.R. The effect of crude-oil aging time and temperature on the rate of water imbibition and long-term recovery by imbibition. *SPE Form. Eval.* **1995**, *10*, 259–266. [CrossRef]
32. Xie, X.; Morrow, N.R. Oil recovery by spontaneous imbibition from weakly water-wet rocks. *Petrophysics* **2001**, *42*, SPWLA-2001-v42n4a1.
33. Mason, G.; Morrow, N.R. Developments in spontaneous imbibition and possibilities for future work. *J. Pet. Sci. Eng.* **2013**, *110*, 268–293. [CrossRef]
34. Jia, P.; Cheng, L.; Huang, S.; Xue, Y.; Clarkson, C.R.; Williams-Kovacs, J.D.; Wang, S.; Wang, D. Dynamic coupling of analytical linear flow solution and numerical fracture model for simulating early-time flowback of fractured tight oil wells (planar fracture and complex fracture network). *J. Pet. Sci. Eng.* **2019**, *177*, 1–23. [CrossRef]
35. He, Y.; Cheng, S.; Li, S.; Huang, Y.; Qin, J.; Hu, L.; Yu, H. A semianalytical methodology to diagnose the locations of underperforming hydraulic fractures through pressure-transient analysis in tight gas reservoir. *SPE J.* **2017**, *22*, 924–939. [CrossRef]
36. Hamidpour, E.; Mirzaei-Paiaman, A.; Masihi, M.; Harimi, B. Experimental study of some important factors on nonwetting phase recovery by cocurrent spontaneous imbibition. *J. Nat. Gas Sci. Eng.* **2015**, *27*, 1213–1228. [CrossRef]
37. Chatzis, I.; Kuntamukkula, M.S.; Morrow, N.R. Effect of capillary number on the microstructure of residual oil in strongly water-wet sandstones. *SPE Reserv. Eng.* **1988**, *3*, 902–912. [CrossRef]
38. Meng, Q.; Liu, H.; Wang, J.; Pang, Z. A symmetry characteristics of oil production by spontaneous imbibition from cores with two ends open, Transp. *Porous Media* **2016**, *113*, 735–751. [CrossRef]
39. Dong, M.; Dullien, F.L.; Zhou, J. Characterization of waterflood saturation profile histories by the 'complete' capillary number. Transp. *Porous Media* **1998**, *31*, 213–237. [CrossRef]
40. Ruth, D.; Bartley, J. A perfect-cross-flow model for two phase flow in porous media. In Proceedings of the International Society of Core Analysts Annual Meeting, Monterey, CA, USA, 22–25 September 2002; pp. 22–25.
41. Dong, M.; Dullien, F.A.; Dai, L.; Li, D. Immiscible displacement in the interacting capillary bundle model part I. Development of interacting capillary bundle model. *Transp. Porous Media* **2005**, *59*, 1–18. [CrossRef]
42. Dong, M.; Dullien, F.A.L.; Dai, L.; Li, D. Immiscible displacement in the interacting capillary bundle model part ii. applications of model and comparison of interacting and non-interacting capillary bundle models. *Transp. Porous Media* **2006**, *63*, 289–304. [CrossRef]
43. Unsal, E.; Mason, G.; Morrow, N.R.; Ruth, D.W. Co-current and counter-current imbibition in independent tubes of non-axisymmetric geometry. *J. Colloid Interface Sci.* **2007**, *306*, 105–117. [CrossRef] [PubMed]
44. Unsal, E.; Mason, G.; Ruth, D.W.; Morrow, N.R. Co-and counter-current spontaneous imbibition into groups of capillary tubes with lateral connections permitting cross-flow. *J. Colloid Interface Sci.* **2007**, *315*, 200–209. [CrossRef] [PubMed]
45. Unsal, E.; Mason, G.; Morrow, N.R.; Ruth, D.W. Bubble snap-off and capillary-back pressure during counter-current spontaneous imbibition into model pores. *Langmuir* **2009**, *25*, 3387–3395. [CrossRef] [PubMed]
46. Das, S.; Waghmare, P.R.; Mitra, S.K. Early Regimes of Capillary Filling. *Phys. Rev. E-Stat. Nonlinear Soft Matter Phys.* **2012**, *86*, 067301. [CrossRef]
47. Gunde, A.; Babadagli, T.; Roy, S.S.; Mitra, S.K. Pore-Scale Interfacial Dynamics and Oil-Water Relative Permeabilities of Capillary Driven Counter-Current Flow in Fractured Porous Media. *J. Pet. Sci. Eng.* **2013**, *103*, 106–114. [CrossRef]
48. Akai, T.; Bijeljic, B.; Blunt, M.J. Wetting Boundary Condition for the Color-Gradient Lattice Boltzmann Method: Validation with Analytical and Experimental Data. *Adv. Water Resour.* **2018**, *116*, 56–66. [CrossRef]